

# Effect of Surfaces on the Performance of CdZnTe Detectors

T. H. Prettyman,<sup>a\*</sup> F. P. Ameduri,<sup>a</sup> A. Burger,<sup>b</sup> J. C. Gregory,<sup>c</sup> M. A. Hoffbauer,<sup>a</sup> P. R. Majerus,<sup>a</sup>  
D. B. Reisenfeld,<sup>a</sup> S. A. Soldner,<sup>d</sup> Cs.Szeles<sup>d</sup>

<sup>a</sup>Los Alamos National Laboratory, Los Alamos, NM 87545, USA

<sup>b</sup>Department of Physics, Center for Photonic Materials and Devices, Nashville, TN 37208, USA

<sup>c</sup>Department of Chemistry, University of Alabama, Huntsville, AL 35899, USA

<sup>d</sup>eV PRODUCTS a division of II-VI Inc., Saxonburg, PA 16056, USA

## ABSTRACT

Surface processing plays a major role in manufacturing CdZnTe semiconductor devices used for radiation detection. We are conducting a thorough, systematic study of surfaces and contacts and their effect on charge transport and signal formation in CdZnTe devices. We are investigating wet chemical processing techniques as well as treatment of surfaces with energetic neutral atoms. Our goal is to develop and implement improved surface treatment methods and device manufacturing techniques for large-volume CdZnTe detectors. In addition, we will determine how surfaces and electrical contacts affect the performance of CdZnTe devices used for radiation detection. In this paper, we will show how surface electronic properties influence carrier transport and signal formation in devices designed to simulate coplanar grid detectors. By altering the surface using a wet chemical process, we will show that charge collection is significantly effected by the conductivity of the surface.

Keywords: CdZnTe, CZT, gamma ray, detector, alpha particle induced charge, coplanar grids, charge collection, surfaces, passivation, contacts

## 1. INTRODUCTION

Surface processing plays a major role in manufacturing CdZnTe semiconductor devices used for radiation detection. Surface properties control many aspects of device operation and performance. The maximum applied bias, for example, is often limited by the conductivity of surface material. Enhanced surface leakage can significantly degrade pulse height resolution, rendering a device unusable for gamma ray spectroscopy. In addition, surface properties can influence the electric field within the device and can have a significant effect on charge transport and signal formation. The effect of surfaces on the electric field is particularly important for devices that use the near pixel effect (e.g. hemispheric devices) and other single-carrier device concepts (e.g. coplanar grids), which are used in the current generation of gamma ray spectrometers. Our goal is to develop and implement improved surface treatment methods and device manufacturing techniques for large-volume CdZnTe detectors. In addition, we will determine how surfaces and electrodes affect the performance of CdZnTe devices used for radiation detection.

We are conducting a thorough, systematic study of surfaces and contacts and their effect on charge transport and signal formation in CdZnTe devices. The product of this effort will be a physics-based model that will accurately predict device performance. This model will be used to engineer improved device structures, and will enable more rapid and less costly development of radiation detectors for nuclear nonproliferation and related applications. In addition, we will investigate a variety of new surface treatment methods, with the goal of improving the quality of processing methods

---

\* Correspondence: Email: [thp@lanl.gov](mailto:thp@lanl.gov); Telephone: 505 667-6449; Fax: 505 665-7395.

used by industry. This information will enable us to develop improved device designs and to develop reliable manufacturing processes.

We are investigating wet chemical processing techniques as well as treatment of surfaces with energetic neutral atoms.<sup>1</sup> Surface analysis techniques (e.g. x-ray photoelectron spectroscopy, atomic force microscopy, etc...) are being used to determine the physical properties of treated surfaces. We are also using electronic characterization methods such as current-voltage measurements and alpha particle induced charge (APIC) measurements to determine the relationship between surface characteristics and device electronic performance. Semiconductor device models will be developed based on the results of these experiments and will be used to guide the selection of processing methods and to design detectors with improved performance for radiation detection.

In this paper, we examine the effect of surface conductivity on charge transport and signal generation within devices with gridded electrodes manufactured from high pressure Bridgman (HPB) material. We first suspected surfaces and contacts had a significant influence on internal electric fields when we attempted to model pulse height spectra for coplanar grid detectors.<sup>2</sup> Because the carrier concentration in bulk CdZnTe material is low ( $<1 \times 10^6 \text{ cm}^{-3}$ ), we assumed that the space charge density was negligible throughout the volume of the device. We found that this assumption grossly underestimated charge collection by the biased anode electrodes in coplanar grid detectors, leading to inaccurate simulations of pulse height spectra.<sup>3,4</sup> A study by Bolotnikov, et al.<sup>5</sup> showed that surface resistance can also influence charge sharing in pixel detectors.

We will show the effect of surface conductivity on the electric field within simplified four-terminal devices that simulate the operation of coplanar grid detectors. The simplified device includes two electrodes separated by a gap, which are designed to model the grid electrodes of a coplanar grid detector. The effect of applying a bias between the two electrodes on the electric field within the device will be examined. By altering the surface using a wet chemical process, we will experimentally show that the internal electric field is significantly effected by the conductivity of the surface.

## 2. THEORY AND MODELING

We are developing physical models that can be applied to predict the performance of CdZnTe devices used for radiation detection. Two-dimensional and in some cases three-dimensional device structures must be modeled. In addition, the full range of semiconductor phenomena must be treated. Compensation mechanisms, carrier transport, contact and surface effects, and position-dependent electronic properties can be modeled using ATLAS, which is a physics-based device simulation package developed for the semiconductor industry.<sup>6</sup> We use an ATLAS module called BLAZE (and BLAZE3D) to model compound semiconductors. BLAZE can model two- and three-dimensional device structures and treats a wide range of semiconductor phenomena, including position dependent band-structure, which could, for example, be used to study the effect of spatial variations in the band gap due to changes in Zn concentration.

We have also developed tools to model the response of devices to radiation interactions. Efficient techniques have been devised to calculate charge pulses produced by radiation interactions, which can be combined with radiation transport models to determine the response of devices to gamma rays and charged particles. An adjoint transport method has been developed to map charge pulses for arbitrary device and electrode geometry.<sup>7,8</sup> This mapping technique will enable us to optimize the design of devices for radiation detection and to interpret charge measurement experiments.

For device design, the steady-state electric field must be calculated using a semiconductor model such as BLAZE. Reliable design of devices for radiation detection requires accurate input parameters for the bulk material, surface and contacts. The bulk resistivity of HPB Cd<sub>1-x</sub>Zn<sub>x</sub>Te (where x=0.1) used for room temperature gamma ray spectroscopy is on the order of  $10^{10} \text{ } \Omega\text{-cm}$ . For x=0.1, the band gap is approximately 1.57 eV, which corresponds to an intrinsic resistivity of  $\sim 6 \times 10^{10} \text{ } \Omega\text{-cm}$  at 300°K. To achieve the resistivity values observed in practice, the Fermi level must be near the middle of the band gap. In addition, the concentration of free carriers in the bulk must be on the order of  $10^5 \text{ cm}^{-3}$ . The compensation mechanism for HPB CdZnTe is described in the literature.<sup>9</sup> It is thought that the material is

compensated by a deep donor level at  $E_v+0.743$  eV, which has a concentration that exceeds the concentration of shallow donors and acceptors in the material. The conductivity of the material is n-type.

For device simulations with BLAZE, we use up to four energy levels to model the electronic properties of the bulk material. The model includes a shallow donor level and a shallow acceptor level. The concentration of the shallow levels is selected such that the difference between the concentration of acceptors and donors is  $<10^{16}$  cm<sup>-3</sup>. The energy of the shallow levels and their cross sections can be adjusted to model trapping and de-trapping of carriers on time scales comparable to the formation of charge pulses. The concentration of the deep donor level is adjusted to fit the measured bulk resistivity of the material. The deep level is also used to control the lifetime of free carriers. Trapping cross sections for electrons and holes are assigned to this level to match experimentally observed lifetimes. A deep level that acts as a hole trap is known to exist at  $E_v+0.735$  eV and is sometimes included in the simulation. The deep acceptor level could influence bulk resistivity and can be used in the model to provide further control over carrier lifetimes and recombination statistics.

Because the bulk free carrier concentration is very low at room temperature, Poisson's equation with the space charge set to zero everywhere within the device is often solved to determine the electric field. This assumption greatly simplifies electric field calculations. However, the model can result in inaccurate estimates of the electric field because it does not consider the effect of surfaces and contacts.

Regions near the surface of semiconductor devices are usually more conductive than the bulk material. Increased conductivity can be caused by the presence of surface states, which cause band-bending resulting in the accumulation of carriers near the surface. Surface roughness also influences the flow of charge on surface. In addition, the surface may consist of dielectric layers that have different properties than the bulk material. Fixed interfacial charge can also be present when an oxide is deposited on the surface. High surface conductivity and fixed interface charge can have a significant effect on the electric field deep (several hundred microns) within the bulk of the material.

We can model the formation of a conductive layer by introducing a surface donor or acceptor state with an energy different from the Fermi level of the bulk material. The result of this process is illustrated in Figure 1. In Figure 1a, an acceptor level was introduced just below the middle of the band-gap. This resulted in an inversion layer (p-type conductivity). In Figure 1b, a donor level was introduced just above the middle of the band-gap. This resulted in an accumulation layer (n-type conductivity). The conductivity of the surface layer can be adjusted by changing the density of the surface state and by adjusting its energy level.

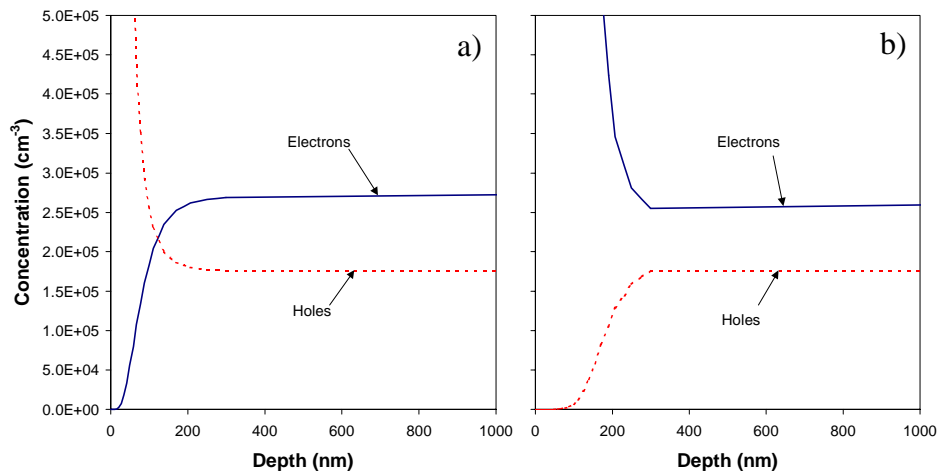


**Figure 1. An inversion layer (a) formed by a surface state that acts as an acceptor at  $E_C-0.8$  eV and an accumulation layer formed by a surface state that acts as a donor at  $E_v+0.8$  eV.**

The effect of a conductive layer on the internal electric field is illustrated in Figure 2 for a device consisting of two electrodes separated by a gap. The electrode on the left is biased positive relative to the one on the right. The electric field in the bulk is established using a full area cathode (at negative bias relative to the two anode electrodes), which is not shown in the figure. In Figure 2a, the electrostatic potential was determined by solving Poisson's equation with the space charge set to zero everywhere in the device. In Figure 2b, the semiconductor model was used to determine the electrostatic potential. The model included enhanced surface conductivity due to the presence of surface states. The addition of a conductive surface enhances charge collection by the biased electrode (the electrode on the left). It should be possible to observe this effect using APIC measurements.

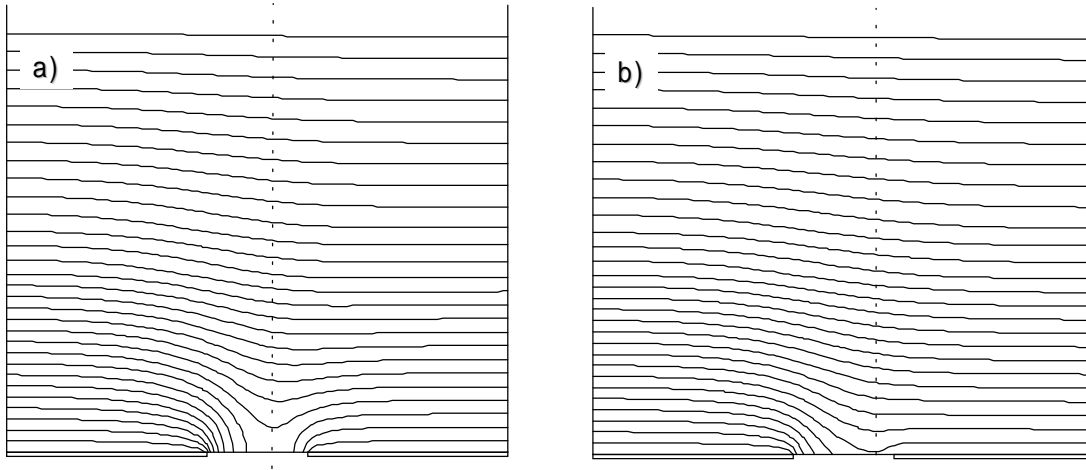


**Figure 2. The electrostatic potential for a device with two electrodes separated by a gap with a differential bias is shown for two cases: a) the solution of Poisson's equation with the space charge set to zero; b) the solution of the semiconductor equations with a conductive surface.**

### 3. EXPERIMENT

We manufactured two devices that simulate the operation of coplanar grid detectors. Both devices were manufactured from single-crystal HPB  $\text{Cd}_{1-x}\text{Zn}_x\text{Te}$  ( $x=0.1$ ) material with uniform electronic properties grown at eV Products. The first device (H15-G1) was manufactured from a  $10 \times 10 \times 5 \text{ mm}^3$  part. The part was previously manufactured as a coplanar grid detector, which was characterized in a previous study.<sup>4</sup> The second device (A16-G1) was manufactured from a  $11 \times 11 \times 6 \text{ mm}^3$  part. A full-area gold contact was deposited on one face of each detector. On the opposite face, platinum contacts consisting of two pads separated by a gap and surrounded by a guard ring were deposited. The pattern is shown in Figure 3.

Prior to deposition of electrodes, the surface was hand polished using 0.25-micron diamond paste. The pattern was sputtered onto the surface through a shadow mask. The thickness of the contact was 1200 Angstroms. Following fabrication, APIC was used to characterize charge transport within the device. Current-voltage characteristics were also measured. The parts were then immersed in an aqueous solution of hydrogen peroxide ( $\text{H}_2\text{O}_2$ ) and ammonium fluoride ( $\text{NH}_4\text{F}$ ) to alter the condition of the surface. Following treatment, the characterization experiments were repeated.

Current-voltage characteristics were determined before and after treatment with the  $\text{H}_2\text{O}_2/\text{NH}_4\text{F}$  solution. The apparatus used to measure leakage current was a computer-controlled system consisting of four Keithley model 617 electrometers. One of the electrometers served as a bias source. The other three were used to make high sensitivity current measurements. Electrical contact to the device was made to the full-area electrode using a conductive pad and to the patterned electrodes with manually adjustable probes. The voltage source was connected to one of the inner electrodes

on the patterned surface. The other electrometers were connected to the remaining electrodes. The probe station was placed in a Tenney Jr. environmental chamber. The Tenney chamber and electrometers were controlled by a personal computer using a Labview<sup>TM</sup> interface.

The Labview software automatically determines resistance at low voltage as a function of temperature. The software adjusts the temperature of the chamber to the desired setting. After a preset delay to allow equilibration, bias is applied to the device. The leakage current is then monitored until it is clear that the temperature within the device has stabilized. This is accomplished by monitoring the leakage current as a function of time using sliding window with 20 samples taken 2 s apart and with absolute convergence criterion of 2 pA. The current is then measured from -1V to -60 mV in 20 mV steps and from -60 mV to 60 mV in 1 mV steps and from 60 mV to 1V in 20 mV steps (a total of 215 measurements). The maximum voltage range was selected so that the nonlinear characteristics of the electrode system (usually back-to-back barriers) could be observed. The low-voltage range (-60 mV to 60 mV) was included so that the resistance of the bulk and surface material could be measured independent of the contact resistance. The resistance is determined by fitting a line to the -60 mV to 60 mV data set.

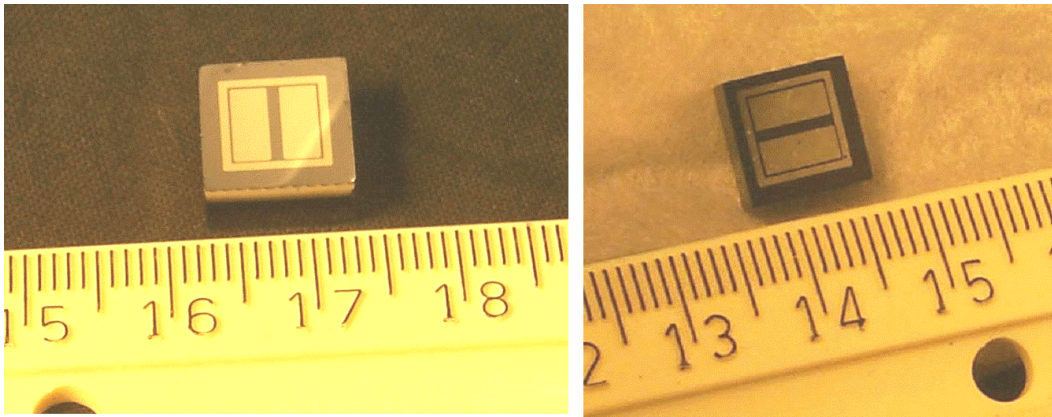


**Figure 3. Devices used to study charge collection are shown. The width of the gap that separates the inner contacts was 838 microns. The device on the right was treated with a  $\text{H}_2\text{O}_2/\text{NH}_4\text{F}$  solution. The surface treatment visibly changes the surface (from a metallic luster to black).**

Charge transport and signal formation was characterized using APIC.<sup>3,4</sup> With APIC, the cathode of the device is exposed to alpha particles from a radioactive source. The alpha particles ionize the material near the cathode. Electrons liberated by the alpha particle interaction are swept away from the cathode by the electric field and drift towards the anode electrode. The holes drift a short distance to the cathode. Because the distance the holes drift is small, the charge pulses induced on the electrodes is caused by the motion of electrons as they drift across the device. The charge pulses are measured using charge sensitive preamplifiers. The shape and amplitude of the charge pulses can be interpreted to determine which electrode collected the charge and the path taken by the electrons to the anode.

A diagram showing the connection of the electrodes to charge sensitive preamplifiers and the orientation of the detector relative to the alpha particle source is given in Figure 4. The CdZnTe device was placed on a conductive pad in a vacuum chamber, which contained an opening approximately 4 mm wide that ran the entire length of the detector in the direction transverse to the gap between the electrodes. The opening allowed the full-area electrode, which served as the cathode, to be exposed to a collimated beam of alpha particles. Alpha particles were emitted by an encapsulated <sup>210</sup>Po (~100  $\mu\text{Ci}$ ) behind a thin window. The average energy of the alpha particles in the beam was ~4 MeV. The chamber was pumped down to <10 microns prior to making measurements to eliminate energy loss in air. The beam was collimated using a slit ~3 mm long by 50 microns wide, which was oriented perpendicular to the opening in the pad.

The width of the beam on the cathode was <800 microns. The source and collimator assembly was mounted on a precision stage, which allowed it to be translated along the length of the detector. The patterned electrodes were connected to charge sensitive preamplifiers using manually adjustable probes. The guard ring was connected to ground.

Data acquisition was automated using Labview™ software. The potential on the cathode ( $V_C$ ) was set to  $-500V$  to establish an electric field within the device of  $\sim 100 V/mm$ . The data acquisition software adjusted the position of the alpha particle source relative to the detector and the differential bias ( $V_B$ ) between the anode electrodes. Measurements were taken in 125-micron increments across the anode electrodes and the gap. At each position, the differential bias was adjusted from 0V to 30V in 5V increments. For each voltage and position, waveforms were acquired for each preamplifier for 250 events. Events were triggered by the cathode signal, which was found to have very uniform amplitude at all positions. The total acquisition time was less than 3 h.

The waveforms were stored in a file for analysis. Waveforms for a recorded event are shown on the right of Figure 4. The differential bias for this event was 15V and the position of the alpha particle source was 704.6 microns from the center of the gap underneath the grounded electrode (A). The waveform for the biased electrode (B) shows evidence of charge sharing. Its slope is positive prior to achieving its final value. The average amplitude of waveforms for each preamplifier was obtained for each position and voltage. Time windows used to determine final values for individual waveforms are shown in Figure 4.

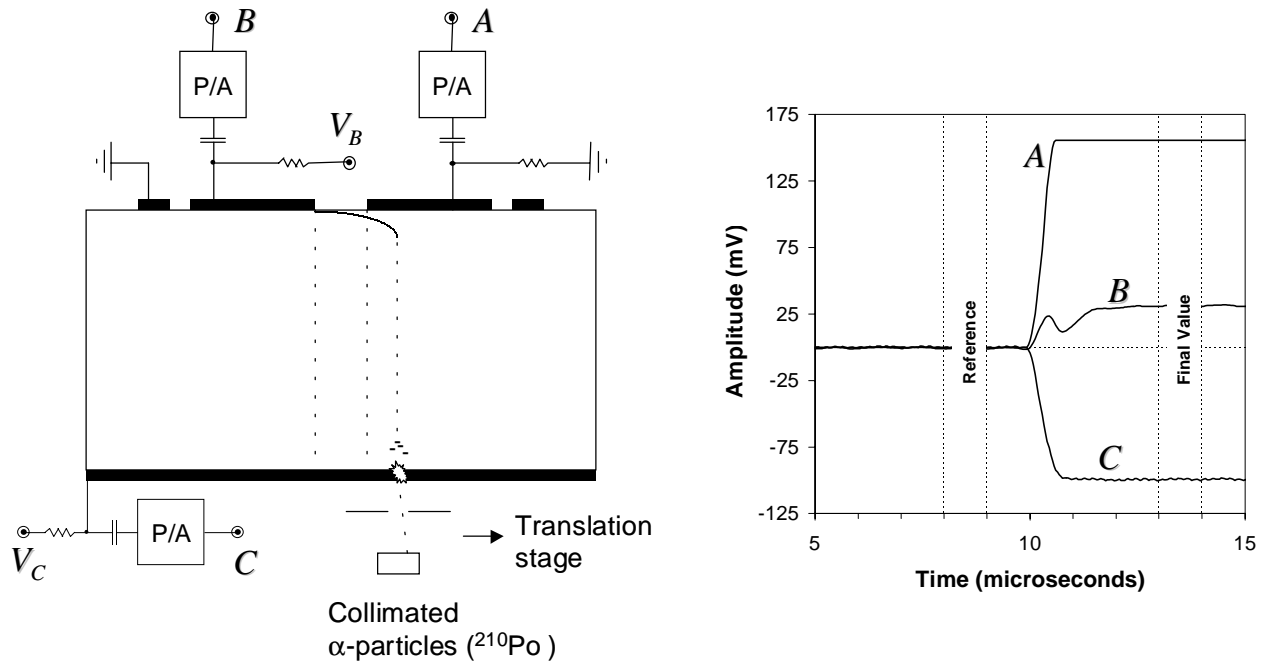


**Figure 4. APIC measurements:** The connection of the electrodes to charge sensitive preamplifiers and the orientation of the detector relative to the alpha particle source is shown on the left. Waveforms for a recorded event are shown on the right. The differential bias for this event was 15V and the position of the alpha particle source was 704.6 microns from the center of the gap underneath the grounded electrode. Time windows used to determine the final amplitude of waveforms relative to the baseline are shown on the right.

## 4. RESULTS

Following treatment with the  $\text{H}_2\text{O}_2/\text{NH}_4\text{F}$  solution, surface resistance was found to drop significantly. For H15-G1, the low-voltage resistance at  $25^\circ\text{C}$  between the two inner electrodes on the patterned surface dropped from  $6.6 \times 10^{10} \Omega$  before treatment to  $1.2 \times 10^9 \Omega$  afterwards. A similar change in surface resistance was observed for A16-G1. In both cases, the bulk current-voltage curve (as measured between one of the inner electrodes on the patterned surface and the full area electrode) did not change. This indicates that treatment with  $\text{H}_2\text{O}_2/\text{NH}_4\text{F}$  solution did not change the electrical properties of the electrodes.

Although treatment with the  $\text{H}_2\text{O}_2/\text{NH}_4\text{F}$  solution has been shown in previous studies to be an effective passivation technique, it does not always result in increased surface resistance.<sup>10</sup> Surface electrical properties following treatment depend on many variables, including surface chemical and structural properties, crystallographic orientation, prior processing steps, and exposure time. In the present study, our goal was to affect a significant change in surface conductivity. The use of  $\text{H}_2\text{O}_2/\text{NH}_4\text{F}$  solution allowed us to modify surface electrical properties without changing the properties of the electrodes. Work is underway to determine the relationship between surface electrical properties, structure, and chemistry.

The average amplitude of waveforms measured by the APIC system for the anode electrodes is shown as a function of position relative to the gap in Figure 5. Note that the anode electrodes are designated A and B in this figure to match the nomenclature in Figure 4. Positive bias was applied to the electrode labeled B. The electrode labeled A was grounded. Note that the amplitude recorded by an electrode was largest when the source is underneath the electrode. The amplitude diminished as the source moved away from the contact. The point at which the amplitudes measured by the two electrodes cross corresponds to the point where charge is shared equally by the two electrodes. At a differential bias of 0V, this point lies directly in the center of the gap. As the bias is increased, the point of charge sharing moves towards the grounded contact. Figure 5 shows the shift in the charge sharing point caused by changing the differential bias from 0V to 30V. The shift in the charge sharing point is plotted in Figure 6 for both detectors as a function of differential bias before and after treatment with the  $\text{H}_2\text{O}_2/\text{NH}_4\text{F}$  solution. The decrease in surface resistance following treatment was accompanied by a large shift in the charge sharing point toward the grounded electrode. The increase in surface conductivity is clearly associated with enhanced collection of charge by the biased electrode.

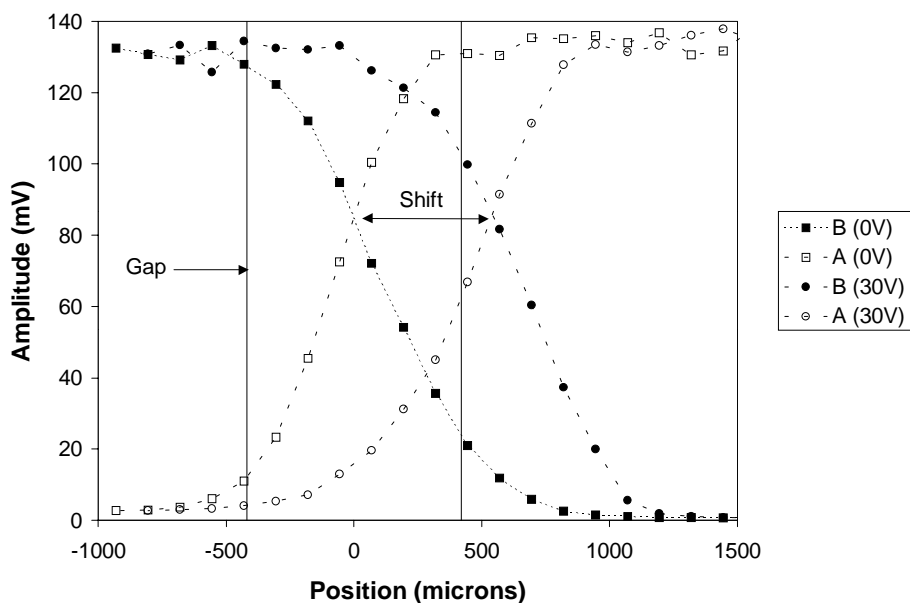
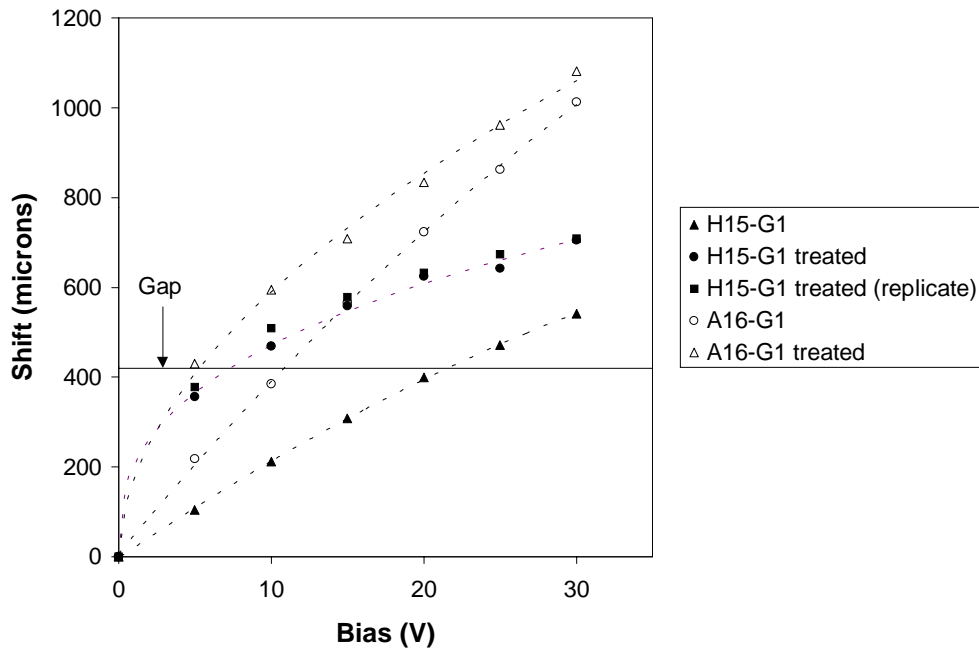


Figure 5. Amplitude of the anode electrode signals as a function of position for 0V and 30V differential bias. The electrode connected to the bias source is labeled B. The grounded electrode is labeled A.



**Figure 6. Shift in the charge sharing point as a function of differential bias before and after treatment with the  $H_2O_2/NH_4F$  solution. The dotted lines are power law fits to the data. Note that one of the cases (labeled replicate) was obtained by removing the device from the APIC system, replacing it, and repeating the experiment. The replicate data set demonstrates that the experiment was reproducible.**

## 5. CONCLUSIONS

We have shown that the presence of a conductive layer at the surface has a significant effect on charge collection and, hence, internal electric fields in CdZnTe devices. This effect was demonstrated experimentally by modifying the surface to increase its conductivity and then observing the location where charge shared equally between two anode electrodes as a function of differential bias for a device designed to simulate coplanar grid operation. The experiment shows that increased surface conductivity results in enhanced charge collection by the biased electrode, which agrees with theoretical predictions.

In the case of coplanar grid devices, the presence of a conductive layer is probably beneficial because complete charge collection by the biased grid electrodes can be achieved at low differential bias. Note that the presence of a conductive layer is usually expected no matter what surface processing techniques are used. Models that do not treat surface conductivity do not predict the shift in the charge sharing point observed experimentally before or after treatment with the  $H_2O_2/NH_4F$  solution. Based on modeling, we believe that increased surface conductivity is also responsible for the high degree of spatial uniformity observed in the response of coplanar grid detectors to alpha particles and gamma rays. Models that do not treat the surface conductive layer do not achieve the uniformity achieved in practice no matter how much bias is applied to the grid electrodes.

Surface electrical properties are expected to have a major effect on the performance of other types of devices used for radiation detection, including planar and hemispheric detectors. Surfaces influence the motion of charge within the device and hence can affect pulse height resolution and detection efficiency. Work is underway to develop quantitative models that can be used to predict the performance of CdZnTe devices. At present, it is believed that the electrical properties of the surface are controlled by a combination of surface states and the presence of a dielectric layer with different electrical properties than the bulk material (e.g. a Te-rich layer). The magnitude of different surface conduction

mechanisms and their relevance to device design is not well understood. Surface analytical techniques are being applied to correlate surface electronic properties with surface structure and composition for different surface processing methods, including wet chemistry and exposure to energetic neutral atoms. This information will be used to develop physical models of the surface that can be used for device design.

## ACKNOWLEDGEMENTS

This work was funded by the Department of Energy Office of Nonproliferation Research and Engineering under contract W-7405-ENG-36.

## REFERENCES

1. T. H. Prettyman, M. A. Hoffbauer, J. A. Rennie, et al., "Performance of CdZnTe detectors passivated with energetic oxygen atoms," Nuclear Instruments and Methods in Physics Research A 422 (1999) 179-184.
2. T. H. Prettyman, C. S. Cooper, P. N. Luke, et al., "Physics-based generation of gamma-ray response functions for CdZnTe detectors," Journal of Radioanalytical Chemistry, Vol. 233, Nos. 1-2 (1998) 257-264.
3. T. H. Prettyman, M. K. Smith, P. N. Luke, M. Amman, J. S. Lee, "Investigation of charge collection in multi-electrode CdZnTe detectors," Proceedings of SPIE (1999).
4. T. H. Prettyman, K. D. Ianakiev, S. A. Soldner, and Cs. Szeles, "Effect of differential bias on the transport of electrons in coplanar grid CdZnTe detectors," Los Alamos National Laboratory document LA-UR-00-2875 (2000), available online at <http://lib-www.lanl.gov/pubs/la-pubs.htm>, submitted to Nuclear Instruments and Methods in Physics Research A.
5. A. E. Bolotnikov, W. R. Cook, F. A. Harrison, et al., "Charge loss between contacts of CdZnTe pixel detectors," Nuclear Instruments and Methods in Physics Research A 432 (1999) 326-331.
6. ATLAS, Silvaco International, Inc., Copyright 1997.
7. T. H. Prettyman, "Method for mapping charge pulses in semiconductor radiation detectors," Nuclear Instruments and Methods in Physics Research A 422 (1-3) (1999) 232-237.
8. T. H. Prettyman, "Theoretical framework for mapping pulse shapes in semiconductor radiation detectors," Nuclear Instruments and Methods in Physics Research A 428 (1) (1999) 72-80.
9. N. Krsmanovic, K. G. Lynn, M. H. Weber, et al., "Electrical compensation in CdTe and Cd<sub>0.9</sub>Zn<sub>0.1</sub>Te by intrinsic defects," Physical Review B 62(24) (2000) 279-282.
10. G. W. Wright, R. B. James, B. A. Brunett, et al., "Evaluation of NH<sub>4</sub>F/H<sub>2</sub>O<sub>2</sub> effectiveness as a surface passivation agent for Cd<sub>1-x</sub>Zn<sub>x</sub>Te crystals," Proceedings of SPIE (2000).